General Disclaimer

One or more of the Following Statements may affect this Document

- This document has been reproduced from the best copy furnished by the organizational source. It is being released in the interest of making available as much information as possible.

- This document may contain data, which exceeds the sheet parameters. It was furnished in this condition by the organizational source and is the best copy available.

- This document may contain tone-on-tone or color graphs, charts and/or pictures, which have been reproduced in black and white.

- This document is paginated as submitted by the original source.

- Portions of this document are not fully legible due to the historical nature of some of the material. However, it is the best reproduction available from the original submission.

SPECKLE NOISE IN DIRECT-DETECTION LIDAR SYSTEMS

by

C. S. Gardner
G. S. Mecherle

RRL Publication No. 495

Technical Report
April 1978

Supported by

Contract No. NASA NSG-5049

NATIONAL AERONAUTICS & SPACE ADMINISTRATION
Goddard Space Flight Center
Greenbelt, Maryland 20771

RADIO RESEARCH LABORATORY
DEPARTMENT OF ELECTRICAL ENGINEERING
COLLEGE OF ENGINEERING
UNIVERSITY OF ILLINOIS
URBANA, ILLINOIS 61801

SPECKLE NOISE IN DIRECT-DETECTION LIDAR SYSTEMS

by

C. S. Gardner
G. S. Mecherle

RRL Publication No. 495

Technical Report
April 1978

Supported by

Contract No. NASA NSG-5049

NATIONAL AERONAUTICS & SPACE ADMINISTRATION
Goddard Space Flight Center
Greenbelt, Maryland 20771

RADIO RESEARCH LABORATORY
DEPARTMENT OF ELECTRICAL ENGINEERING
COLLEGE OF ENGINEERING
UNIVERSITY OF ILLINOIS
URBANA, ILLINOIS 61801

TABLE OF CONTENTS

LIST OF FIGURES

LIST OF TABLES

I. INTRODUCTION

In a recent report we developed and summarized the basic equations describing speckle noise in satellite based lidar systems [1]. The speckle noise power in direct detection systems was found to be a complicated function of the electrical characteristics of the receiver electronics, receiver aperture size and shape, laser pulse shape, laser radiation pattern and characteristics of the scattering medium. In this report the speckle noise will be evaluated from some typical lidar systems. The governing equations, which were developed in [1], are summarized in the remainder of this section. In Section II the mutual intensity function of the speckle pattern is calculated in terms of the laser radiation modes. Typical laser pulses are modeled in Section III, and in Sections IV and V simplified expressions for the speckle noise power are derived. The signal-to-speckle-noise ratios for some proposed lidar systems are evaluated in Section VI.

The variance of the signal at the output of the receiver illustrated in Figure 1 can be written in the form [1]

$$\mathrm{Var}(S) = \delta E(S) + \frac{(1 + P^2)}{2M_S M_T} E^2(S) \qquad \text{(I-1)}$$

where E(S) is the average signal. The first term on the right-hand side of Equation (I-1) is the shot noise component, while the second term is the speckle noise component. The magnitude of the speckle noise is affected by the size of the telescope aperture, bandwidth of the receiver electronics and polarization characteristics of the signal. In Equation (I-1) P is the degree of signal polarization ($0 \leq P \leq 1$), M_S is the effective number of spatial correlation cells seen by the receiver aperture, and M_T is the effective number of temporal correlation cells seen by the receiver's

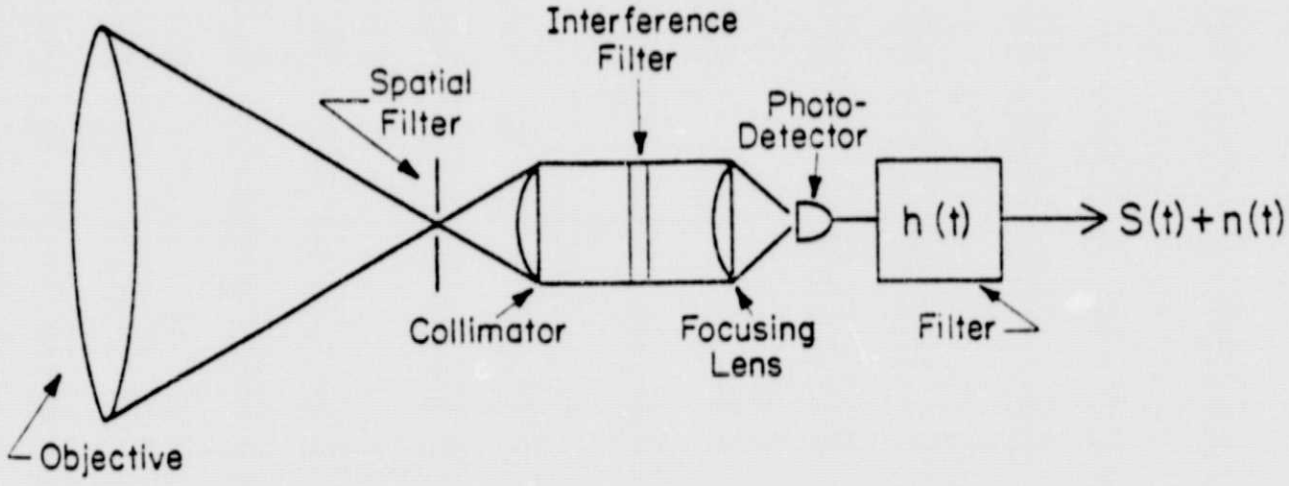

Figure 1. Receiving system model.

electrical filter. M_S and M_T depend on the characteristics of the signal mutual intensity function $\tilde{J}_A$ which in most cases is separable.

$$\tilde{J}_A(\underline{r},\tau) = \tilde{J}_S(\underline{r})\ \tilde{J}_T(\tau) \quad . \tag{I-2}$$

Using Equation (I-2), M_S, M_T, and δ can be written as

$$M_S = \frac{\left\{|\tilde{J}_S(0)| \int d^2\underline{r} W(\underline{r})\right\}^2}{\int d^2\underline{r} |\tilde{J}_S(\underline{r})|^2 R_W(\underline{r})} \tag{I-3}$$

$$M_T = \frac{\left\{|\tilde{J}_T(0)| R_p(0) \int_{-\infty}^{\infty} d\tau h(\tau)\right\}^2}{\int_{-\infty}^{\infty} d\tau |\tilde{J}_T(\tau)|^2 R_p^2(\tau)\ R_h(\tau)} \tag{I-4}$$

$$\delta = \frac{R_h(0)}{\int_{-\infty}^{\infty} d\tau h(\tau)} \tag{I-5}$$

$$R_W(\underline{r}) = \int_{-\infty}^{\infty} d^2\underline{\rho}\ W(\underline{\rho})\ W^*(\underline{\rho} + \underline{r}) \tag{I-6}$$

$$R_p(\tau) = \int_{-\infty}^{\infty} dt\ P(t)\ P(t + \tau) \tag{I-7}$$

$$R_h(\tau) = \int_{-\infty}^{\infty} dt\ h(t)\ h(t + \tau) \quad . \tag{I-8}$$

$W(\underline{r})$ is the receiver aperture weighting function, $P(t)$ the laser pulse shape and $h(t)$ the impulse response of the receiver's electrical filter. R_W, R_p and R_h are their associated autocorrelation functions. The expression for M_T is valid only for particulate scattering. For rough surface scattering the laser pulse has no effect so that M_T becomes

$$M_T = \frac{\left(|\tilde{J}_T(0)| \int_{-\infty}^{\infty} d\tau h(\tau)\right)^2}{\int_{-\infty}^{\infty} d\tau |\tilde{J}_T(\tau)|^2 R_h(\tau)} \quad . \tag{I-9}$$

Closed form expressions for M_S and M_T are usually difficult to calculate when typical system functions are substituted into Equations (I-3) and (I-4). Therefore, it is sometimes convenient to consider the limiting expressions when M_S and M_T are large. M_S is approximately one when the receiving aperture diameter is small compared to the spatial correlation length of the received signal. When the aperture is large, M_S can be approximated by the formula

$$M_S \approx \frac{\left(\int d^2\underline{r} W(\underline{r})\right)^2}{R_w(0)} \quad \frac{|\tilde{J}_S(0)|^2}{\int d^2\underline{r} |\tilde{J}_S(\underline{r})|^2} \quad . \tag{I-10}$$

Similarly, M_T is approximately one when the bandwidth of h is large compared to the temporal coherence bandwidth of the received signal. When the bandwidth of h is small, M_T can be approximated by

$$M_T \approx \frac{\left(\int_{-\infty}^{\infty} d\tau h(\tau)\right)^2}{R_h(0)} \quad \frac{|\tilde{J}_T(0)|^2 R_p^2(0)}{\int_{-\infty}^{\infty} d\tau |\tilde{J}_T(\tau)|^2 R_p^2(\tau)} \quad . \tag{I-11}$$

Goodman [2] has shown that the spatial component of the mutual intensity function is related to the intensity distribution which illuminates the scattering medium. If we denote by $E(\underline{r},z)$ the complex optical signal incident on the scattering volume, then $|\tilde{J}_S|^2$ is given by

$$\frac{|\tilde{J}_S(\underline{r})|^2}{|\tilde{J}_S(0)|^2} = \frac{\left|\int d^2\underline{\rho} |E(\underline{\rho},z)|^2 \exp\left(i \frac{2\pi}{\lambda z} \underline{r} \cdot \underline{\rho}\right)\right|^2}{\left|\int d^2\underline{\rho} |E(\underline{\rho},z)|^2\right|^2} \quad . \tag{I-12}$$

λ is the signal wavelength and z is the distance from the scattering medium

to the receiving telescope. Equation (I-12) is valid in both the Fresnel and Fraunhofer scattering zones provided the microstructure of the scattering medium is unresolvable by the receiving telescope.

For a coherent laser source, the temporal component of the mutual intensity function is related to the statistics of the fluctuations in the velocity of the scattering particles. If the particle velocity fluctuations are Gaussian, $|\tilde{J}_T|^2$ is given by [1]

$$\frac{|\tilde{J}_T(\tau)|^2}{|\tilde{J}_T(0)|^2} = \exp\left[- 2 \left(\frac{2\pi}{\lambda}\right)^2 \left| \tau \int_0^\tau d\xi (1 - \xi/\tau)\, R_{\Delta v}(\xi) \right| \right] . \qquad \text{(I-13)}$$

$R_{\Delta v}$ is the velocity correlation function. The Gaussian assumption is valid for Brownian motion and for turbulent flow which may be found in clouds and smoke plumes. It is interesting to evaluate (I-13) for the limiting cases where τ is either large or small compared to the velocity correlation time. If we let τ_v denote the velocity correlation time, (I-13) becomes

$$\frac{|\tilde{J}_T(\tau)|^2}{|\tilde{J}_T(0)|^2} = \begin{cases} \exp\left[- \left(\frac{2\pi}{\lambda}\right)^2 \langle \Delta v^2 \rangle \tau^2 \right] & \tau << \tau_v \\ \exp\left[- 2 \left(\frac{2\pi}{\lambda}\right)^2 |\tau| \int_0^\infty d\xi\, R_{\Delta v}(\xi) \right] & \tau >> \tau_v \end{cases} . \qquad \text{(I-14)}$$

For particles suspended in a turbulent flow, the velocity correlation is usually quite long ($\sim$ ms) compared to the observation time so that $|\tilde{J}_T|^2$ takes on the Gaussian form. The velocity correlation time is usually negligible for Brownian motion and in this case $|\tilde{J}_T|^2$ takes on the exponential form which gives rise to the familiar Lorentzian spectrum.

For rough surface scattering the temporal coherence time of the scattered signal (τ_c) is determined by the source coherence time (τ_{sc}).

For scattering by an ensemble of particles, τ_c may depend both on the source coherence time and the inverse Doppler linewidth of the scattering molecule (τ_d) [1].

The Doppler linewidth is given by [6]

$$\frac{1}{\tau_d} = \Delta\nu_D = 2\nu_0\sqrt{\frac{2kT}{Mc^2}\ln 2} \qquad \text{(I-15)}$$

where

ν_0 = center frequency of radiation

k = Boltzmann's constant

T = temperature (°K)

M = mass of the molecule

c = velocity of light.

For T = 300°K, τ_d becomes

$$\tau_d = \frac{\lambda_0\sqrt{\text{At. Wt.}}}{3705.44} \qquad \text{(I-16)}$$

where At. Wt. = the atomic weight of the scattering molecule.

When scattering from resonant molecules, τ_c is equal to τ_d. When the scattering mechanism is Rayleigh, τ_c becomes

$$\tau_c = (\tau_{sc}^{-2} + \tau_d^{-2})^{-1/2} \quad . \qquad \text{(I-17)}$$

In the following Sections M_S and M_T are evaluated for typical lidar system functions. Effects such as high-order laser modes and annular receiving apertures are considered.

II. LASER MODE EFFECTS ON $|\tilde{J}_S|$

In Cartesian coordinates the propagation modes of laser radiation are described by the well-known Gauss-Hermite functions [3].

$$E_{mn}(x,y,z) = \mathcal{E}(z)\, H_m\left(\sqrt{2}\,\frac{x}{\omega}\right) H_n\left(\sqrt{2}\,\frac{y}{\omega}\right) \exp\left[-(x^2+y^2)\left(\frac{1}{\omega^2}+\frac{ik}{2R}\right) + i\,\psi_{mn}\right] \quad \text{(II-1)}$$

$$\omega^2(z) = \omega_0^2\left[1+\left(\frac{\lambda z}{\pi\omega_0^2}\right)^2\right] \quad \text{(II-2)}$$

$$R(z) = z\left[1+\left(\frac{\pi\omega_0^2}{\lambda z}\right)^2\right] \quad \text{(II-3)}$$

$$\psi_{mn}(z) = (m+n+1)\tan^{-1}\left(\frac{\lambda z}{\pi\omega_0^2}\right) . \quad \text{(II-4)}$$

The field distribution given by (II-1) corresponds to the TEM_{mn} mode. $\mathcal{E}$ is a complex function independent of x and y, H_m is a Hermite polynomial and ω_0 is the beam radius of the fundamental mode at $z = 0$. The far-field divergence angle of the fundamental Gaussian mode is

$$\theta_T = \frac{\lambda}{\pi\omega_0} . \quad \text{(II-5)}$$

Equations (II-1) - (II-5) correspond to the case where the beam is collimated at the $z = 0$ plane. For situations where the laser is not collimated, the origin of the z-axis must be shifted and ω_0 adjusted in Equations (II-1) - (II-5) to give the correct phase front curvature and beam radius at the laser coordinates [3].

The spatial component of the mutual intensity function can be calculated for an arbitrary mode by substituting (II-1) into (I-12) and integrating [4]

$$\frac{|\tilde{J}_S(\underline{r})|^2}{|\tilde{J}_S(0)|^2} = \left[L_m\left(\frac{\pi^2\omega^2}{\lambda^2 z^2} x^2\right) L_n\left(\frac{\pi^2\omega^2}{\lambda^2 z^2} y^2\right) \right]^2 \exp\left[-\left(\frac{\pi\omega}{\lambda z}\right)^2 (x^2 + y^2) \right] \qquad \text{(II-6)}$$

where L_m is a Laguerre polynomial. Equation (II-6) will be used in the following sections to evaluate the effects of high-order laser modes on the speckle statistics.

III. LASER PULSE EFFECTS ON R_p

To evaluate M_T it is necessary to obtain a functional expression for P(t), the laser pulse shape. If the pulse is symmetric in time, it may be possible to approximate it by a Gaussian distribution, while the Gamma distribution can often be used to represent asymmetric pulse shapes.

Both the Gaussian and Gamma distribution pulses are completely characterized by the full width at half-maximum (FWHM) and by the time coordinate at which the peak occurs (T_p). Fortunately, these two parameters are also easy to measure in the laboratory. However, since optical detectors respond to intensity, $P^2(t)$ is the function that is usually measured. Thus, it is necessary to fit the distribution to the pulse intensity profile, and then take the square root to find P(t), the pulse amplitude.

For a Gaussian-shaped pulse, we let

$$P(t) = \frac{1}{\sqrt{2\pi}\,\tau_p} e^{-t^2/2\tau_p^2} \qquad \text{(III-1)}$$

where

$$\tau_p = \frac{1}{\sqrt{8 \ln 2}} (\text{FWHM}) = 0.425(\text{FWHM}) \quad . \qquad \text{(III-2)}$$

For a Gamma distribution pulse, we let

$$P(t) = \begin{cases} \dfrac{c^{b+1}}{\Gamma(b+1)} t^b e^{-ct} & t > 0 \\ 0 & \text{otherwise} \end{cases} \qquad \text{(III-3)}$$

where

$$\text{mean} = \int_0^\infty dt\ t\ P(t) = \frac{b+1}{c} \tag{III-4}$$

$$\text{RMS width} = \left(\int_0^\infty dt\ t^2\ P(t) - (\text{mean})^2 \right)^{1/2} = \frac{\sqrt{b+1}}{c} \tag{III-5}$$

$$\text{peak} = T_p = b/c \quad . \tag{III-6}$$

Although it is possible to determine b and c from the mean and RMS width using Equations (III-4) and (III-5), these parameters are not as easily measured as T_p and FWHM.

$$b = \begin{cases} \dfrac{T_p}{FWHM} \ln 2 & \dfrac{FWHM}{T_p} > 60 \\ \text{Figure 2} & 1.1 < \dfrac{FWHM}{T_p} < 5 \\ (8 \ln 2) \left(\dfrac{T_p}{FWHM} \right)^2 & \dfrac{FWHM}{T_p} < 2.5 \end{cases} \tag{III-7}$$

$$c = b/T_p \quad . \tag{III-8}$$

For the Gaussian distribution the autocorrelation function is given by

$$R_p(t) = \frac{1}{2\sqrt{\pi}\ \tau_p} e^{-t^2/4\tau_p^2} \tag{III-9}$$

$$R_p(0) = \frac{1}{2\sqrt{\pi}\ \tau_p} \tag{III-10}$$

and for the Gamma distribution the autocorrelation function is [5, p. 322]

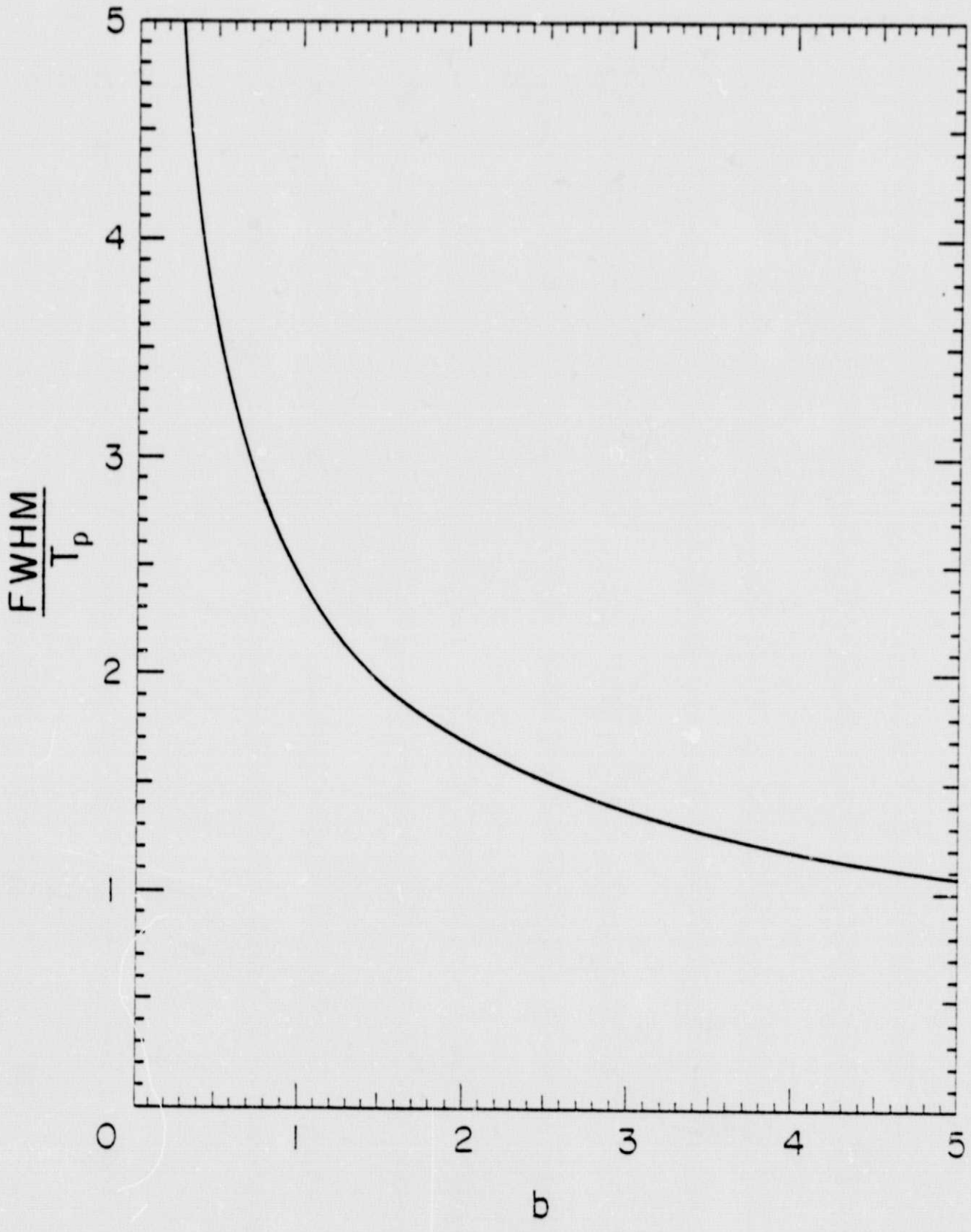

Figure 2. FWHM/T_p versus b for 1.1 < FWHM/T_p < 5.

$$R_p(t) = \frac{c^{b+3/2}}{\sqrt{\pi}\,\Gamma(b+1)} \left(\frac{t}{2}\right)^{b+1/2} K_{b+1/2}(ct) \qquad \text{(III-11)}$$

$$R_p(0) = \frac{c}{2\sqrt{\pi}} \frac{\Gamma(b+1/2)}{\Gamma(b+1)} \qquad \text{(III-12)}$$

where $K_{b+1/2}(ct)$ is a modified Bessel function.

IV. EVALUATION OF M_S FOR TYPICAL SYSTEM FUNCTIONS

A. $|\tilde{J}_S|$ Gaussian, W Gaussian

As seen in Section I, M_S is dependent on the receiving aperture weighting function, $W(\underline{r})$, and the spatial component of the mutual intensity function, $\tilde{J}_S(\underline{r})$. It is instructive to consider the case for which both the aperture and mutual intensity functions are Gaussian, since this is one of the few cases that a closed-form expression for M_S can be derived exactly.

The Gaussian form for the mutual intensity is given by

$$\left|\frac{\tilde{J}_S(\underline{r})}{\tilde{J}_S(0)}\right|^2 = e^{-r^2/2\rho_c^2} \tag{IV-1}$$

where ρ_c is the transverse spatial coherence length of the signal. The spatial coherence length can be expressed in terms of the transmitter divergence angle, or in terms of the laser spot radius (see Section II).

$$\rho_c = \frac{\lambda}{\sqrt{2}\ \pi\Theta_T} \tag{IV-2}$$

$$\rho_c = \frac{\lambda z}{\sqrt{2}\ \pi\omega(z)} \quad . \tag{IV-3}$$

Θ_T is the laser transmitter divergence angle and $\omega(z)$ is the radius of the laser spot at the scattering medium. As given in Equation (II-2), the spot size is

$$\omega^2(z) = \omega_0^2\left[1 + \left(\frac{\lambda z}{\pi\omega_0^2}\right)^2\right] \tag{IV-4}$$

where ω_0 is the beam radius at $z = 0$.

The Gaussian receiver aperture is modeled as

$$W(\underline{r}) = e^{-r^2/R^2} \tag{IV-5}$$

where R is the receiver aperture radius. The receiving aperture autocorrelation is given by

$$R_W(\underline{r}) = \frac{\pi R^2}{2} e^{-r^2/2R^2} \quad . \tag{IV-6}$$

For W and $|\tilde{J}_S|$ Gaussian, Equation (I-3) for M_S becomes

$$M_S = 1 + R^2/\rho_c^2 \tag{IV-7}$$

From Equation (I-10), the large aperture approximation for M_S is given by

$$M_S \simeq \frac{\left(\int d^2\underline{r} W(\underline{r})\right)^2}{R_W(0)} \quad \frac{|\tilde{J}_S(0)|^2}{\int d^2\underline{r} |\tilde{J}_S(\underline{r})|^2} \quad . \tag{IV-8}$$

For large values of R/ρ_c, M_S is large, and Equation (IV-8) gives

$$M_S \simeq R^2/\rho_c^2 \quad . \tag{IV-9}$$

B. $|\tilde{J}_S|$ Gaussian, W Annular

In general, $W(\underline{r})$ will be a circular annular aperture as in a Cassegrain telescope. Let R_1 be the outer radius of the aperture, R_2 the radius inside which the aperture is obscured, and $\gamma = R_2/R_1$ the obscuration ratio. To evaluate M_S, it was necessary to numerically integrate Equation (I-3). Plots of M_S versus R_1/ρ_c are given in Figure 3 for γ equal to zero and one-half. From Equation (IV-8), the large M_S approximation becomes

$$M_S \simeq \frac{R_1^2(1 - \gamma^2)}{2\rho_c^2} \quad . \tag{IV-10}$$

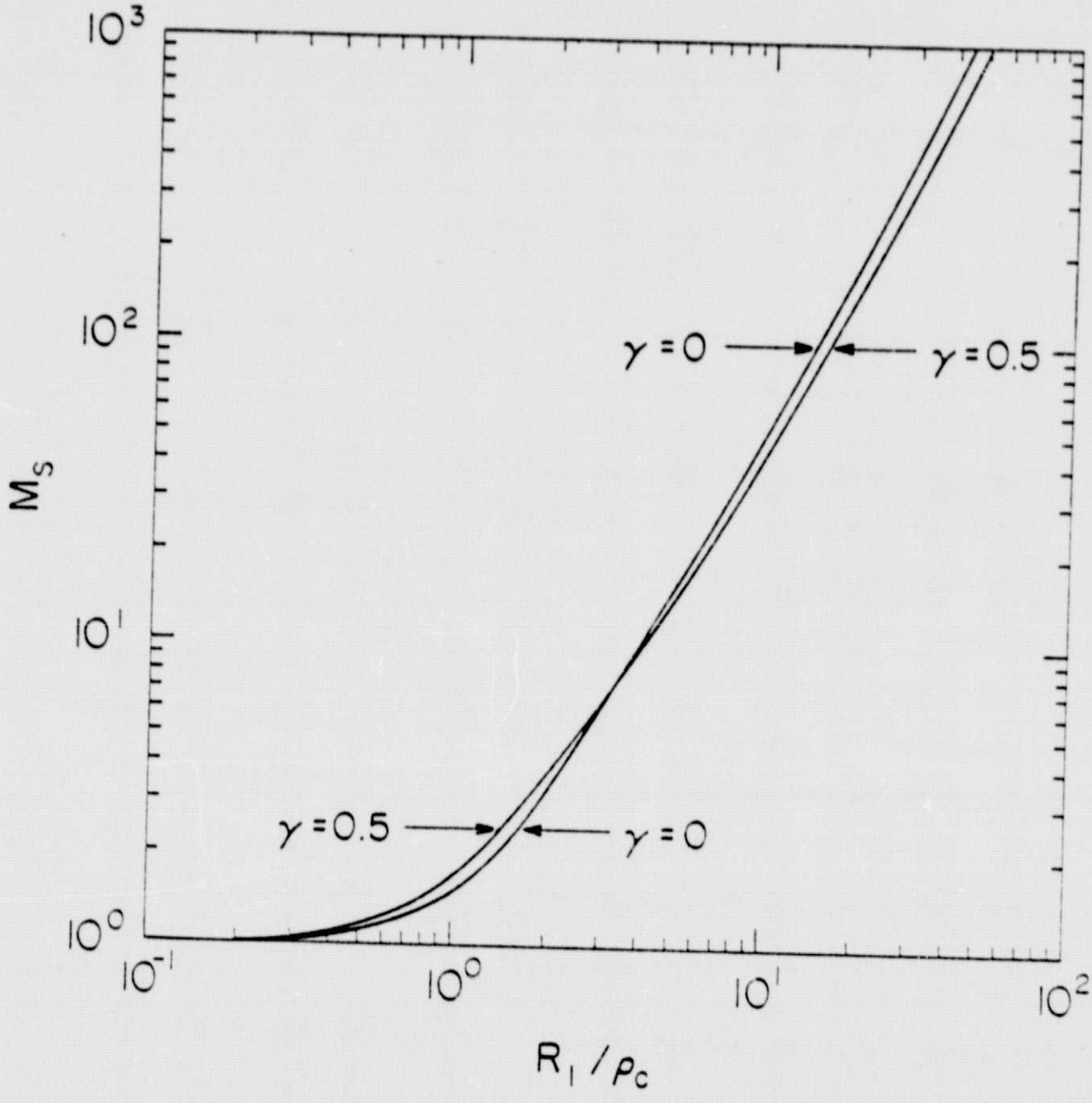

Figure 3. M_S versus R_1/ρ_c for $.1 < R_1/\rho_c < 100$.

Since the receiver aperture weighting function for annular apertures is that $W = 1$ inside the aperture and $W = 0$ outside the aperture, $W(\underline{r}) = W^2(\underline{r})$. Thus, $R_W(0) = \int d^2\underline{r} W(\underline{r})$ so that the large aperture approximation for M_S (Equation (IV-8)) simplifies to

$$M_S \approx \frac{\int d^2\underline{r} W(\underline{r})}{\int d^2\underline{r} \left| \tilde{J}_S(\underline{r}) / \tilde{J}_S(0) \right|^2} \quad . \tag{IV-11}$$

In this case M_S is just the ratio of the receiver area to the effective area of the square of the normalized mutual intensity function.

C. Large Aperture Approximation for Arbitrary Laser Modes

Although it was not possible to obtain an exact expression for M_S for an arbitrary TEM_{mn} transverse mode, it is nevertheless quite useful to evaluate the large M_S approximation for the TEM_{mn} mode.

Referring to Equation (IV-8) for large M_S, in Cartesian coordinates, it is necessary to evaluate $\iint dx\, dy \left| \tilde{J}_S / \tilde{J}_S(0) \right|^2$. For the TEM_{mn} mode the square of the mutual intensity function is given by Equation (II-6).

$$\frac{\left| \tilde{J}_S(\underline{r}) \right|^2}{\left| \tilde{J}_S(0) \right|^2} = \left[L_m\left(\frac{\pi^2\omega^2}{\lambda^2 z^2} x^2 \right) L_n\left(\frac{\pi^2\omega^2}{\lambda^2 z^2} y^2 \right) \right]^2 \exp\left[-\left(\frac{\pi\omega}{\lambda z} \right)^2 (x^2 + y^2) \right] \quad . \tag{IV-12}$$

The two spatial dimensions may be separated, yielding two integrals of the form

$$\int_{-\infty}^{\infty} dx \left[L_m\left(\frac{\pi^2\omega^2}{\lambda^2 z^2} x^2 \right) \right]^2 \exp\left[-\left(\frac{\pi\omega}{\lambda z} \right)^2 x^2 \right] \quad . \tag{IV-13}$$

This integral can be evaluated by making a change of variables

$$v = \frac{\pi\omega}{\lambda z} x$$

and expanding one of the Laguerre polynomials into the form [5, p. 1037]

$$L_m(v^2) = \sum_{k=0}^{m} (-1)^k \begin{pmatrix} m \\ m-k \end{pmatrix} \frac{v^{2k}}{k!} \quad . \tag{IV-14}$$

With another change of variables $u = v^2$, Equation (IV-13) becomes

$$\frac{\lambda z}{\pi\omega} \sum_{k=0}^{m} (-1)^k \begin{pmatrix} m \\ m-k \end{pmatrix} \frac{1}{k!} \frac{1}{2} \int_{-\infty}^{\infty} du\, u^{k-1/2} L_m(u)\, e^{-u} \quad . \tag{IV-15}$$

The integral in (IV-15) can be found in [5, p. 845], yielding the result

$$\int_{-\infty}^{\infty}\int_{-\infty}^{\infty} dx\, dy \left| \tilde{J}_S / \tilde{J}_S(0) \right|^2 = \frac{\lambda^2 z^2}{\pi\omega^2} \gamma_m \gamma_n = 2\pi\rho_c^2 \gamma_m \gamma_n \tag{IV-16}$$

where

$$\gamma_m = \frac{1}{2^{2m}} \sum_{k=0}^{m} \frac{1}{2^{2k}} \begin{pmatrix} 2m-2k \\ m-k \end{pmatrix} \begin{pmatrix} 2k \\ k \end{pmatrix}^2 \tag{IV-17}$$

$$\gamma_n = \frac{1}{2^{2n}} \sum_{k=0}^{n} \frac{1}{2^{2k}} \begin{pmatrix} 2n-2k \\ n-k \end{pmatrix} \begin{pmatrix} 2k \\ k \end{pmatrix}^2 \quad . \tag{IV-18}$$

Thus, for any TEM_{mn} transverse mode, the integrated mutual intensity is scaled by γ_m and γ_n compared to the Gaussian case ($\gamma_0 = 1$). The total integrated mutual intensity can be expressed as the sum of the integrated intensities of all transverse modes present, each scaled by the appropriate γ_m and γ_n.* However, if the mode structure of the laser transmitter is unknown, the Gaussian mode will give the worst case estimate for M_S, since a higher order mode will result in a reduced integrated intensity and consequently an increased M_S. Tabulated values of γ_m are given below.

*This assumes that the transverse modes are statistically independent.

TABLE 1. TABULATED VALUES OF γ_m

m	γ_m
0	1.0000
1	.7500
2	.6406
3	.5742
4	.5279
5	.4930
6	.4653
7	.4426
8	.4235
9	.4070
10	.3927
20	.3076
40	.2381

If we insert Equations (IV-16) - (IV-18) into Equation (IV-8), the large M_S approximation for a Gaussian aperture and TEM_{mn} mode becomes

$$M_S \approx \frac{R^2}{\rho_c^2 \gamma_m \gamma_n} \quad . \tag{IV-19}$$

Similarly, the large M_S approximation for an annular aperture and TEM_{mn} mode yields

$$M_S \approx \frac{R_1^2(1 - \gamma^2)}{2\rho_c^2 \gamma_m \gamma_n} \quad . \tag{IV-20}$$

The results are summarized in Table 2.

TABLE 2. SUMMARY OF M_S RESULTS

$W(\underline{r})$	$\lvert\tilde{J}_S(\underline{r})\rvert$	M_S	
		Exact	Large M_S Limit
Gaussian Equation (IV-5)	Gaussian Equation (IV-1)	$1 + R^2/\rho_c^2$	R^2/ρ_c^2
Annular	Gaussian	Figure 3	$\frac{R_1^2(1 - \gamma^2)}{2\rho_c^2}$
Gaussian	TEM_{mn} Equation (IV-12)	--	$\frac{R^2}{\rho_c^2 \gamma_m \gamma_n}$
Annular	TEM_{mn}	--	$\frac{R_1^2(1 - \gamma^2)}{2\rho_c^2 \gamma_m \gamma_n}$

R = Gaussian aperture radius

R_1 = outer radius of annular aperture

γ = obscuration ratio of annular aperture

ρ_c = transverse spatial coherence length of signal (Equations (IV-2) and (IV-3))

γ_m and γ_n = the integrated intensity scaling factors for the TEM_{mn} mode (Equations (IV-17) and (IV-18) and Table 1).

V. EVALUATION OF M_T FOR TYPICAL SYSTEM FUNCTIONS

Referring to Equation (I-4) for M_T, we need to know what functional forms $|\tilde{J}_T(t)|$, P(t), and h(t) will assume for realistic systems. It was shown in Section I that $|\tilde{J}_T|$ will usually have Gaussian or exponential form, and in Section III that P can be represented by the Gaussian or Gamma distributions. The electrical filter h(t) will usually be an integrator or ideal low-pass filter; however, it is also useful to consider the Gaussian low-pass filter.

A. P Gaussian, $|\tilde{J}_T|$ Gaussian

Insight may be gained as to how these parameters interact by considering the case where they are all Gaussian.

$$\left|\frac{\tilde{J}_T(t)}{\tilde{J}_T(0)}\right|^2 = e^{-t^2/2\tau_c^2} \tag{V-1}$$

$$P(t) = \frac{1}{\sqrt{2\pi}\,\tau_p} e^{-t^2/2\tau_p^2} \tag{V-2}$$

$$R_p^2(t) = \frac{1}{4\pi\tau_p^2} e^{-t^2/2\tau_p^2} \tag{V-3}$$

$$h(t) = e^{-t^2B^2} \tag{V-4}$$

$$R_h(t) = \frac{\sqrt{\pi}}{\sqrt{2}\,B} e^{-t^2B^2/2} \tag{V-5}$$

$$R_h(0) = \frac{\sqrt{\pi}}{\sqrt{2}\,B} \tag{V-6}$$

$$\int_{-\infty}^{\infty} dt\ h(t) = \sqrt{\pi}/B \qquad \text{(V-7)}$$

τ_c is the speckle coherence time, τ_p is the laser pulse width, and B is the filter bandwidth.

Inserting (V-1) - (V-7) into Equation (I-4) for M_T yields

$$M_T = \left[1 + \frac{1}{B^2\tau_c^2} + \frac{1}{B^2\tau_p^2}\right]^{1/2} . \qquad \text{(V-8)}$$

We find that M_T is inversely related to the filter bandwidth, pulse width, and coherence time. The large M_T approximation (Equation (I-11)) is given by

$$M_T \approx \frac{\left[\int_{-\infty}^{\infty} dt\ h(t)\right]^2}{R_h(0)} \quad \frac{|\tilde{J}_T(0)|^2\ R_p^2(0)}{\int_{-\infty}^{\infty} dt\,|\tilde{J}_T(t)|^2\ R_p^2(t)} . \qquad \text{(V-9)}$$

Using (V-I) - (V-7) for all Gaussian functions, Equation (V-9) becomes

$$M_T \approx \frac{1}{B}\left[\frac{1}{\tau_p^2} + \frac{1}{\tau_c^2}\right]^{1/2} . \qquad \text{(V-10)}$$

M_T can also be evaluated exactly for the cases where $|\tilde{J}_T|$ and P are Gaussian and h is an ideal low-pass filter or integrator. For h an integrator, we have

$$h(t) = \begin{cases} 1 & |t| \le 1/2B \\ 0 & \text{otherwise} \end{cases} \qquad \text{(V-11)}$$

$$R_h(t) = \begin{cases} 1/B - |t| & |t| \le 1/B \\ 0 & \text{otherwise} \end{cases} \qquad \text{(V-12)}$$

$$R_h(0) = 1/B \qquad \text{(V-13)}$$

$$\int_{-\infty}^{\infty} dt\ h(t) = 1/B \quad . \tag{V-14}$$

Note that 1/B is the integration time. For convenience, we will define the parameter ψ.

$$\psi = \frac{1}{B}\left(\frac{1}{\tau_p^2} + \frac{1}{\tau_c^2}\right)^{1/2} \quad . \tag{V-15}$$

Then, using Equations (V-11) - (V-15) and Equations (V-1) - (V-3) for P and $|\tilde{J}_T|$ Gaussian, M_T is given by [5, p. 306]

$$M_T = \frac{\psi^2/2}{\sqrt{\pi/2}\ \psi\ \mathrm{erf}(\psi/2) + \exp(-\psi^2/2) - 1} \tag{V-16}$$

where erf(x) is the error function. For large ψ, M_T is large, and Equations (V-9) and (V-16) become

$$M_T = \frac{\psi}{\sqrt{2\pi}} \quad . \tag{V-17}$$

For the case in which h is an ideal low-pass filter, we have

$$h(f) = \begin{cases} 1 & |f| \leq B \\ 0 & \text{otherwise} \end{cases} \tag{V-18}$$

$$R_h(t) = h(t) = 2B\ \mathrm{sinc}\ 2Bt \tag{V-19}$$

$$R_h(0) = 2B \tag{V-20}$$

$$\int_{-\infty}^{\infty} dt\ h(t) = 1 \tag{V-21}$$

where B is the filter bandwidth. Equation (I-4) for M_T contains the integral of the product of a Gaussian and a sinc function, which can be evaluated to obtain [5, p. 495]

$$M_T = \frac{(\psi/2\sqrt{2\pi})\ \exp(2\pi^2/\psi^2)}{{}_1F_1(1,1.5,2\pi^2/\psi^2)} \qquad \text{(V-22)}$$

where ${}_1F_1$ is a hypergeometric function. For large ψ, Equations (V-9) and (V-22) become

$$M_T \approx \frac{\psi}{2\sqrt{2\pi}} \quad . \qquad \text{(V-23)}$$

Plots of M_T versus ψ for $|\tilde{J}_T|$ and P Gaussian are presented in Figure 4 for the cases where h is an integrator, ideal low-pass filter and Gaussian low-pass filter.

B. P Gaussian, $|\tilde{J}_T|$ Exponential

Now we consider the case in which P is Gaussian, $|\tilde{J}_T|$ is exponential, and h is Gaussian. $|\tilde{J}_T|$ is given by

$$\left|\frac{\tilde{J}_T(t)}{\tilde{J}_T(0)}\right|^2 = e^{-|t|/2\tau_c} \qquad \text{(V-24)}$$

where τ_c is the speckle coherence time. Inserting (V-24) and (V-2) - (V-7) into Equation (I-4) for M_T, we obtain the integral of a Gaussian multiplied by an exponential. This can be evaluated [5, p. 307], and M_T is given by

$$M_T = \frac{\sqrt{1 + 1/B^2\tau_p^2}\ \exp\left(\dfrac{-1}{8(B^2\tau_c^2 + \tau_c^2/\tau_p^2)}\right)}{\operatorname{erfc}\left(\dfrac{1}{2\sqrt{2}\sqrt{B^2\tau_c^2 + \tau_c^2/\tau_p^2}}\right)} \qquad \text{(V-25)}$$

where $\operatorname{erfc}(z) = 1 - \operatorname{erf}(z)$ is the complementary error function. For large M_T, Equation (V-9) contains the integral of the product of a Gaussian and an exponential, which becomes [5, p. 307]

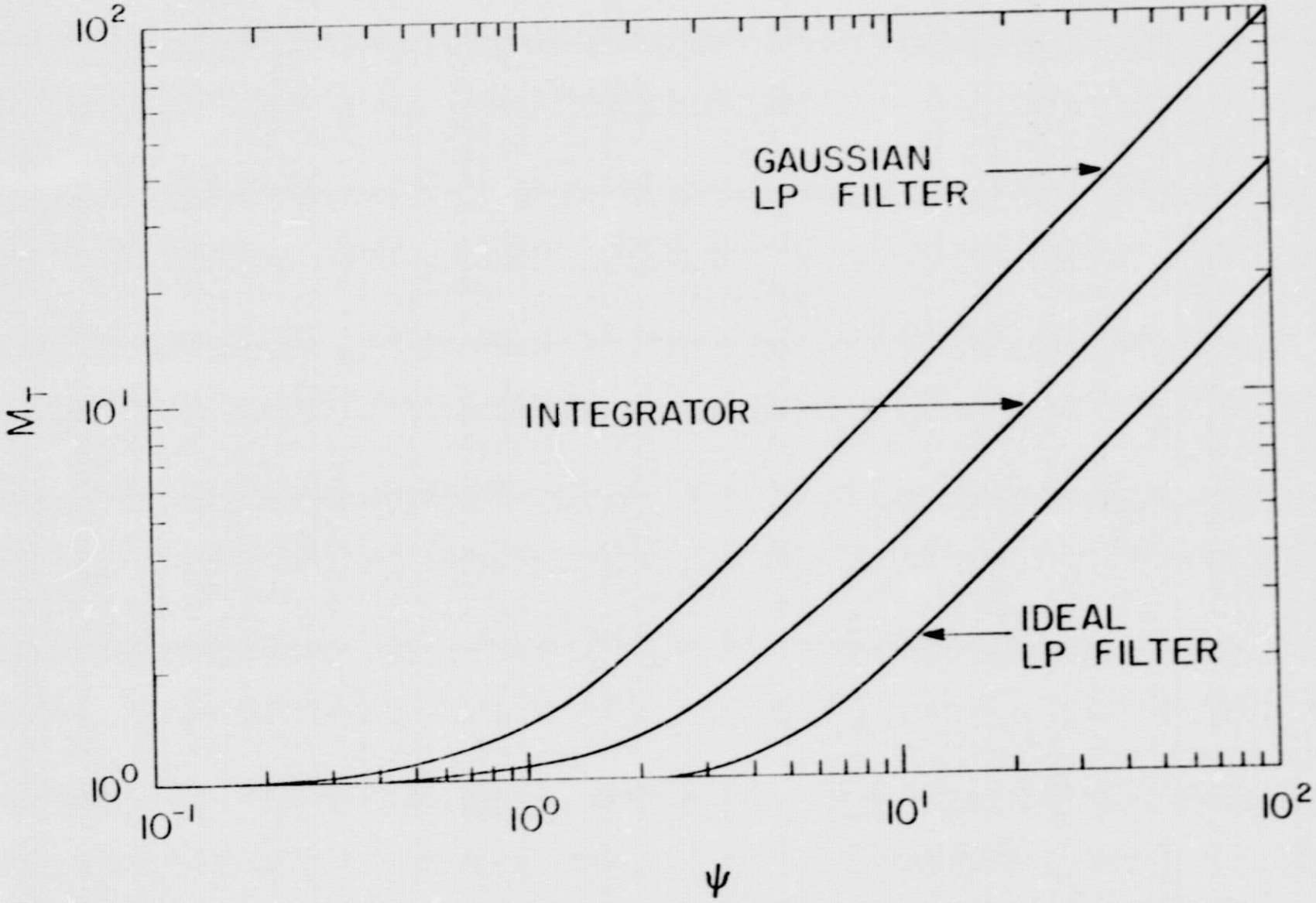

Figure 4. M_T versus ϕ for $.1 < \phi < 100$.

$$M_T \approx \frac{1}{B\tau_p Q} \tag{V-26}$$

where the function Q is given by

$$Q = \exp\left(\frac{\tau_p^2}{8\tau_c^2}\right) \operatorname{erfc}\left(\frac{\tau_p}{2\sqrt{2}\ \tau_c}\right) . \tag{V-27}$$

Q is plotted versus τ_p/τ_c in Figure 4. For large τ_p/τ_c, Q becomes approximately equal to

$$Q \approx \frac{2\sqrt{2}\ \tau_c}{\sqrt{\pi}\ \tau_p} . \tag{V-28}$$

For small τ_p/τ_c, Q is approximately equal to one.

For the case in which P is Gaussian, $|\tilde{J}_T|$ is exponential, and h is an integrator, we insert Equations (V-2), (V-3), (V-11) - (V-14), and (V-24) into Equation (I-4) for M_T. Completing the square in the exponent and making a change of variables gives two integrals of the form

$$\int_{u_1}^{u_2} du\ e^{-u^2} \tag{V-29}$$

$$\int_{u_1}^{u_2} du\ ue^{-u^2} . \tag{V-30}$$

Equation (V-29) results in the difference of two error functions [5, p. 306], while (V-30) is an exact differential. After considerable manipulation, we obtain the result

$$M_T = \left\{ \sqrt{2\pi}\, B\tau_p \left(1 + \frac{B\tau_p^2}{2\tau_c}\right) \exp\left(\frac{\tau_p^2}{8\tau_c^2}\right) \left[\operatorname{erf}\left(\frac{1}{\sqrt{2}\, B\tau_p} + \frac{\tau_p}{2\sqrt{2}\,\tau_c}\right) - \operatorname{erf}\left(\frac{\tau_p}{2\sqrt{2}\,\tau_c}\right) \right] + 2B^2\tau_p^2 \left(\exp\left(\frac{-1}{2B^2\tau_p^2} - \frac{1}{2B\tau_c} \right) - 1 \right) \right\}^{-1} . \qquad \text{(V-31)}$$

For large M_T, Equation (V-9) again is the product of a Gaussian and an exponential, which is evaluated to yield

$$M_T \approx \frac{1}{\sqrt{2\pi}\, B\tau_p\, Q} \qquad \text{(V-32)}$$

where $Q = \exp(\tau_p^2/8\tau_c^2)\ \operatorname{erfc}(\tau_p/2\sqrt{2}\,\tau_c)$ and is plotted in Figure 5 versus τ_p/τ_c.

For P Gaussian, $|\tilde{J}_T|$ exponential, and h an ideal low-pass filter, Equation (I-4) for M_T becomes

$$M_T = \left\{ \frac{2}{\pi} \int_0^\infty \exp\left(\frac{-t^2}{2\tau_p^2} - \frac{t}{2\tau_c} \right) \frac{\sin 2B\pi t}{t}\, dt \right\}^{-1} . \qquad \text{(V-33)}$$

Equation (V-33) must be integrated numerically to obtain exact values for M_T. However, Equation (V-9) for large M_T can still be evaluated to give

$$M_T \approx \frac{1}{2\sqrt{2\pi}\, B\tau_p\, Q} \qquad \text{(V-34)}$$

where again $Q = \exp(\tau_p^2/8\tau_c^2)\ \operatorname{erfc}(\tau_p/2\sqrt{2}\,\tau_c)$ is plotted in Figure 5 versus τ_p/τ_c.

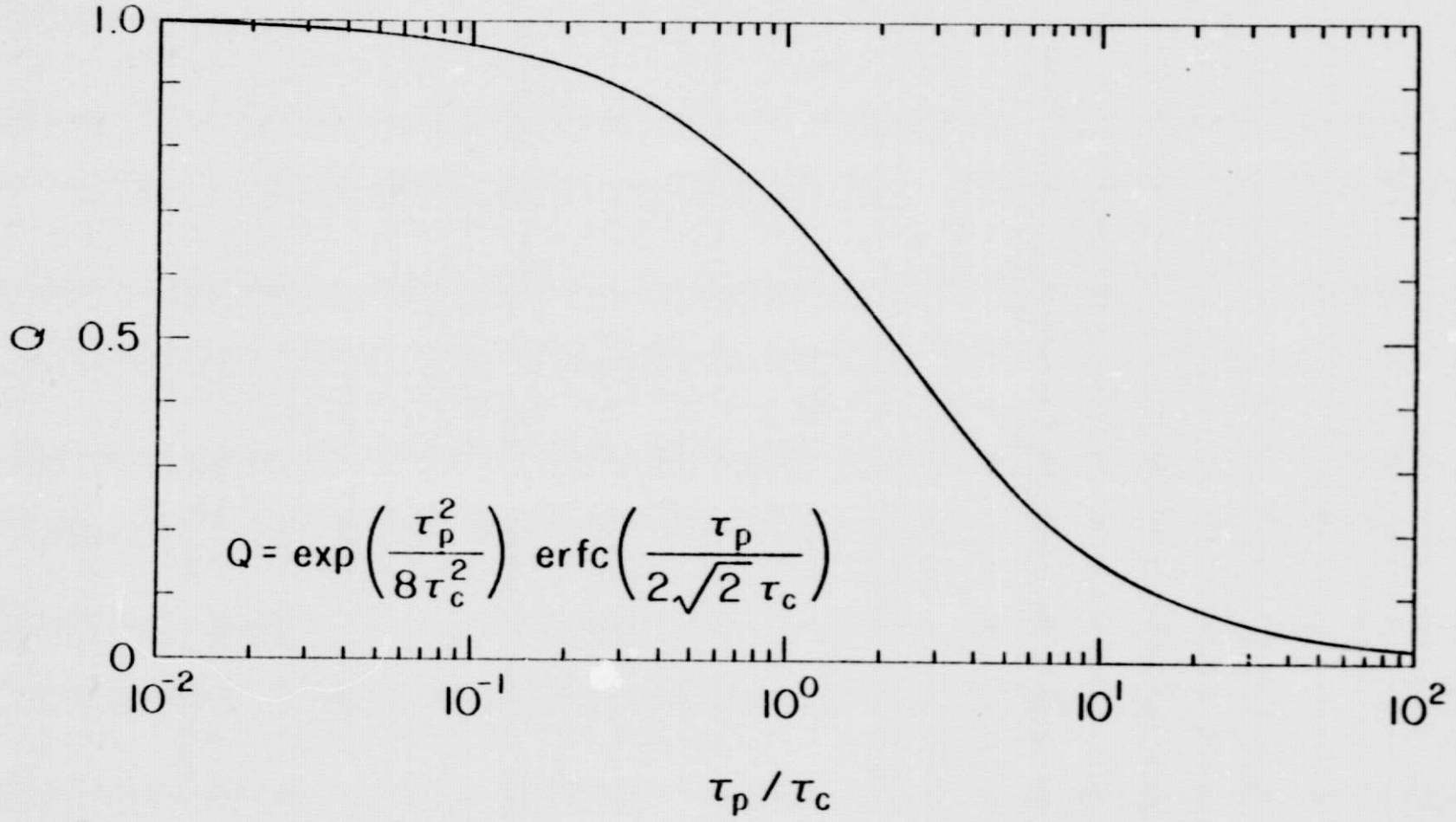

Figure 5. $Q = \exp(\tau_p^2/8\tau_c^2)\ \mathrm{erfc}(\tau_p/2\sqrt{2}\tau_c)$ versus τ_p/τ_c for $.01 < \tau_p/\tau_c < 100.$

C. Large M_T Approximation for P(t) Modeled by a Gamma Distribution

When P(t) is represented by a Gamma distribution (see Section III), exact values of M_T must be obtained by numerical integration. However, the large M_T approximation can be manipulated into a relatively simple form.

For most system resolution requirements, h will be slowly varying compared to the pulse width and coherence time. Consequently, we may use Equation (V-9) for large M_T and treat the dependence on h as a separate factor. Equation (V-9) can be written as

$$M_T \approx \mu_h \, M_T' \tag{V-35}$$

where

$$\mu_h = \frac{\left\{\int_{-\infty}^{\infty} dt \; h(t)\right\}^2}{R_h(0)} \tag{V-36}$$

$$M_T' = \frac{|\tilde{J}_T(0)|^2 \; R_p^2(0)}{\int_{-\infty}^{\infty} dt |\tilde{J}_T(t)|^2 \; R_p^2(t)} \quad . \tag{V-37}$$

Values of μ_h for a Gaussian low-pass filter, integrator, and ideal low-pass filter are tabulated below.

TABLE 3. TABULATED VALUES OF μ_h

h(t)	μ_h
Gaussian low-pass filter	$\sqrt{2\pi}/B$
Integrator	$1/B$
Ideal low-pass filter	$1/2B$

When P(t) is represented by a Gamma distribution, Equation (V-37) must be integrated numerically. But we are able to obtain closed-form expressions for M_T' whenever either the pulse width or coherence time is short. If $\tau_p \ll \tau_c$, $|\tilde{J}_T|^2$ can be evaluated at zero and removed outside the integral in Equation (V-37). Then M_T' becomes

$$M_T' \approx \frac{R_p^2(0)}{\int_{-\infty}^{\infty} dt\ R_p^2(t)} \quad . \tag{V-38}$$

For P(t) Gamma, $R_p(t)$ is given by Equation (III-11), so that Equation (V-38) yields

$$M_T' \approx \frac{c}{2\sqrt{\pi}} \frac{\Gamma^2(b + 1/2)}{\Gamma^2(b + 1)} \frac{\Gamma(2b + 2)}{\Gamma\left(\frac{4b + 3}{2}\right)} \tag{V-39}$$

where b and c are related to the peak and width of the laser pulse using Equations (III-7) and (III-8).

If $\tau_c \ll \tau_p$, $R_p^2(t)$ can be evaluated at zero and removed outside the integral in Equation (V-37). Then M_T' is given by

$$M_T' \approx \frac{|\tilde{J}_T(0)|^2}{\int_{-\infty}^{\infty} dt\ |\tilde{J}_T(t)|^2} \quad . \tag{V-40}$$

If $|\tilde{J}_T|$ is Gaussian, Equation (V-40) becomes

$$M_T' \approx \frac{1}{\sqrt{2\pi}\ \tau_c} \quad . \tag{V-41}$$

If $|\tilde{J}_T|$ is exponential, Equation (V-40) becomes

$$M_T' \approx \frac{1}{4\tau_c} \quad . \tag{V-42}$$

The results for M_T are summarized in Table 4, and functional forms used to evaluate M_T are given in Table 5.

TABLE 4. SUMMARY OF M_T RESULTS

Explanation of Terms

Γ = Gamma Distribution

G = Gaussian Distribution

Exp = Exponential Distribution

Int = Integrator

LPF = Low-Pass Filter

$\psi = (1/\tau_p^2 + 1/\tau_c^2)^{1/2}/B$

τ_p = pulse width of laser

τ_c = coherence time of received signal

B = bandwidth of receiver electrical filter

$Q = \exp(\tau_p^2/8\tau_c^2)\ \mathrm{erfc}(\tau_p/2\sqrt{2}\ \tau_c)$ (Figure 5)

b and c = parameters which characterize the Gamma distribution (Equations (III-4) and (III-8)).

TABLE 4. (CONTINUED)

P(t)	$\tilde{J}_T(t)$	h(t)	M_T Exact	Large M_T Limit
G	G	G LPF	$[1 + \phi^2]^{1/2}$	$M_T = \phi$
G	G	Int.	$\dfrac{\phi^2/2}{\sqrt{\pi/2}\ \phi\ \mathrm{erf}(\phi/\sqrt{2}) + \exp(-\phi^2/2) - 1}$	$M_T = \phi/\sqrt{2\pi}$
G	G	Ideal LPF	$\dfrac{(\phi/2\sqrt{2\pi})\ \exp(2\pi^2/\phi^2)}{{}_1F_1(1,1.5,2\pi^2/\phi^2)}$	$M_T = \phi/2\sqrt{2\pi}$
G	Exp.	G LPF	$\dfrac{\sqrt{1 + 1/B^2\tau_p^2}\ \exp\left(\dfrac{-1}{8(B^2\tau_c^2 + \tau_c^2/\tau_p^2)}\right)}{\mathrm{erfc}\left(\dfrac{1}{2\sqrt{2}\sqrt{B^2\tau_c^2 + \tau_c^2/\tau_p^2}}\right)}$	$M_T = \dfrac{1}{B\tau_p Q}$
G	Exp.	Int.	$\left\{\sqrt{2\pi}\ B\tau_p\left(1 + \dfrac{B\tau_p^2}{2\tau_c}\right)\exp\left(\dfrac{\tau_p^2}{8\tau_c^2}\right)\left[\mathrm{erf}\left(\dfrac{1}{\sqrt{2}\ B\tau_p} + \dfrac{\tau_p}{2\sqrt{2}\ \tau_c}\right) - \mathrm{erf}\left(\dfrac{\tau_p}{2\sqrt{2}\ \tau_c}\right)\right] + 2B^2\tau_p^2\left[\exp\left(\dfrac{-1}{2B^2\tau_p^2} - \dfrac{1}{2B\tau_c}\right) - 1\right]\right\}^{-1}$	$M_T = \dfrac{1}{\sqrt{2\pi}\ B\tau_p Q}$
G	Exp.	Ideal LPF	$\left[\dfrac{2}{\pi}\int_0^\infty \exp\left(\dfrac{-t^2}{2\tau_p^2} - \dfrac{t}{2\tau_c}\right)\dfrac{\sin 2B\pi t}{t}\,dt\right]^{-1}$	$M_T = \dfrac{1}{2\sqrt{2\pi}\ B\tau_p Q}$

TABLE 4. (CONTINUED)

P(t)	$\tilde{J}_T(t)$	h(t)	M_T Exact	Large M_T Limit	
				$\tau_p \ll \tau_c$	$\tau_c \ll \tau_p$
Γ	G	G LPF	--	$\frac{c}{\sqrt{2}\,B} \frac{\Gamma^2(b+1/2)\,\Gamma(2b+2)}{\Gamma^2(b+1)\,\Gamma\left(\frac{4b+3}{2}\right)}$	$\frac{1}{B\tau_c}$
Γ	G	Int.	--	$\frac{c}{2\sqrt{\pi}\,B} \frac{\Gamma^2(b+1/2)\,\Gamma(2b+2)}{\Gamma^2(b+1)\,\Gamma\left(\frac{4b+3}{2}\right)}$	$\frac{1}{\sqrt{2\pi}\,B\tau_c}$
Γ	G	Ideal LPF	--	$\frac{c}{4\sqrt{\pi}\,B} \frac{\Gamma^2(b+1/2)\,\Gamma(2b+2)}{\Gamma^2(b+1)\,\Gamma\left(\frac{4b+3}{2}\right)}$	$\frac{1}{\sqrt{8\pi}\,B\tau_c}$
Γ	Exp.	G LPF	--	$\frac{c}{\sqrt{2}\,B} \frac{\Gamma^2(b+1/2)\,\Gamma(2b+2)}{\Gamma^2(b+1)\,\Gamma\left(\frac{4b+3}{2}\right)}$	$\frac{\sqrt{\pi}}{2\sqrt{2}\,B\tau_c}$
Γ	Exp.	Int.	--	$\frac{c}{2\sqrt{\pi}\,B} \frac{\Gamma^2(b+1/2)\,\Gamma(2b+2)}{\Gamma^2(b+1)\,\Gamma\left(\frac{4b+3}{2}\right)}$	$\frac{1}{4B\tau_c}$
Γ	Exp.	Ideal LPF	--	$\frac{c}{4\sqrt{\pi}\,B} \frac{\Gamma^2(b+1/2)\,\Gamma(2b+2)}{\Gamma^2(b+1)\,\Gamma\left(\frac{4b+3}{2}\right)}$	$\frac{1}{8B\tau_c}$

TABLE 5. FUNCTIONAL FORMS USED TO EVALUATE M_T

Function	P(t)	$\lvert\tilde{J}_T(t)/\tilde{J}_T(0)\rvert^2$	h(t)
Gaussian	$\frac{1}{\sqrt{2\pi}\,\tau_p} e^{-t^2/2\tau_p^2}$	$e^{-t^2/2\tau_c^2}$	$e^{-t^2B^2}$
Exponential	$\begin{cases} ce^{-ct} & t > 0 \\ 0 & \text{otherwise} \end{cases}$	$e^{-\lvert t\rvert/2\tau_c}$	--
Ideal Low-Pass Filter	--	--	2B sinc 2Bt
Integrator	--	--	$\begin{cases} 1 & \lvert t\rvert \leq \frac{1}{2B} \\ 0 & \text{otherwise} \end{cases}$
Gamma Distribution	$\begin{cases} \frac{c^{b+1}}{\Gamma(b+1)} t^b e^{-ct} & t > 0 \\ 0 & \text{otherwise} \end{cases}$	--	--

τ_c = coherence time of received signal

τ_p = laser pulse width (Equation (III-2))

B = bandwidth of electrical filter

b and c = parameters which characterize the Gamma distribution. (Equations (III-4) - (III-8))

VI. SIGNAL-TO-NOISE RATIO FOR REPRESENTATIVE LIDAR SYSTEMS

To evaluate the quality of lidar data for a given system, we must evaluate the signal-to-noise power ratio (SNR), which is given by [1]

$$\mathrm{SNR} = \frac{E(S)^2}{\mathrm{Var}(S) + \mathrm{Var}(N)} \quad .$$

Under strong signal conditions, the signal speckle noise dominates and the SNR becomes

$$\mathrm{SNR} \approx \frac{2M_S M_T}{(1 + P^2)} \quad .$$

A summary of the SNR calculations for various systems is given in Table 6. For these systems it was assumed that the laser is transmitting in the fundamental Gaussian mode, the received field is polarized in one component, the pulse is Gaussian, the electrical filter is an integrator, and the obscuration ratio of the circular receiving aperture is 0.25.

TABLE 6. SNR FOR REPRESENTATIVE SYSTEMS

		λ (μm)	θ_T (mr)	ρ_c (m)	R_1 (m)	M_S	B(MHz)	τ_p (ns)	τ_c (sec)	ψ	M_T	SNR
1.	OH-O_3 OH	.282	0.25	3.20×10^{-4}	0.15	1.03×10^{5}	1.0	4.25	3.14×10^{-10}	3193	1274	1.31×10^{8}
	"	.305	0.25	2.54×10^{-4}	0.15	1.64×10^{5}	1.0	4.25	3.39×10^{-10}	2959	1180	1.94×10^{8}
	O_3	.355	0.25	2.75×10^{-4}	0.15	1.40×10^{5}	1.0	127.5	6.64×10^{-10}	1506	601	8.41×10^{7}
2.	HF	.5321	1.0	1.20×10^{-4}	0.09	2.64×10^{5}	10.0	4.25	10^{-3}	23.53	9.8	2.59×10^{6}
3.	CO_2	9.2	0.5	4.14×10^{-3}	0.09	220	20.0	42.5	1.65×10^{-8}	3.25	1.72	378
		10.8	0.5	4.86×10^{-3}	0.09	160	20.0	42.5	1.93×10^{-8}	2.85	1.58	253
4.	ESA	1.06	0.5	4.77×10^{-4}	0.25	1.29×10^{5}	200	8.5	10^{-3}	.588	1.02	1.32×10^{5}
		.5321	0.5	2.40×10^{-4}	0.25	5.09×10^{5}	200	8.5	10^{-3}	.588	1.02	5.19×10^{5}
		.589	0.5	2.65×10^{-4}	0.25	4.17×10^{5}	200	8.5	10^{-3}	.598	1.02	4.25×10^{5}
5.	H_2O	.7	0.6	2.62×10^{-4}	0.55	2.07×10^{6}	0.33	8.5	8.01×10^{-10}	3800	1516	3.14×10^{9}
		1.0	0.6	3.75×10^{-4}	0.55	1.01×10^{6}	0.33	8.5	1.14×10^{-9}	2682	1070	1.08×10^{9}

λ = wavelength of laser signal; θ_T = laser transmitter divergence angle; ρ_c = transverse spatial coherence length of signal; R_1 = outer radius of annular aperture; M_S = number of correlation cells seen by receiver; B = bandwidth of electrical filter; τ_p = width of received pulse; τ_c = coherence time of received signal; $\psi = (1/\tau_p^2 + 1/\tau_c^2)^{1/2}/B$; M_T = number of temporal correlation cells seen by receiver; SNR = signal-to-noise power ratio of received signal